Variability at intermediate depths at the equator in the Atlantic Ocean in 2000–06: annual cycle, equatorial deep jets, and intraseasonal meridional velocity fluctuations.

Lucia Bunge, Christine Provost, Bach Lien Hua, Annie Kartavtseff

Variability at Intermediate Depths at the Equator in the Atlantic Ocean in 2000–06: Annual Cycle, Equatorial Deep Jets, and Intraseasonal Meridional Velocity Fluctuations

LUCIA BUNGE* AND CHRISTINE PROVOST

LOCEAN, UMR 7159, Université Pierre et Marie Curie, Paris, France

BACH LIEN HUA

Laboratoire de Physique des Océans, CNRS-IFREMER-UBO, Plouzané, France

ANNIE KARTAVTSEFF

LOCEAN, UMR 7159, Université Pierre et Marie Curie, Paris, France

(Manuscript received 23 February 2007, in final form 9 January 2008)

ABSTRACT

Time series of high vertical resolution current meter measurements between 600-m and 1800-m depths on the equator in the Atlantic were obtained at two locations, 10° and 23°W. The measurements have a time span of almost 7 years (2000–06) and provide insights into the temporal scales and vertical structure of variability at intermediate depths. Variability in the zonal velocity component records is dominated by semiannual, annual, and interannual fluctuations. At semiannual and annual periodicities, vertical scales are large, on the order of 2000 stretched meters (sm), and show upward phase propagation. In contrast, interannual variability is associated with small vertical scale flows, called equatorial deep jets (EDJs), presenting downward phase propagation most of the time. Fitting a plane wave to these small vertical-scale flows leads to velocity amplitude, vertical scale, and temporal scale estimates of 8 (normalized) cm s^{-1}, 440 sm, and 4.4 yr. However, this plane wave cannot explain all the variability presenting small vertical scales. Indeed, the data suggest that, along with a seasonal cycle of much larger vertical scale, different features with EDJ vertical scale coexist, with the possibility of a semipermanent eastward jet at around 1500 sm. Variability in the meridional velocity component is dominated by intraseasonal fluctuations. In addition, at 23°W, the meridional component shows low-frequency flows that may be due to the interaction of zonal fluctuations with the Mid-Atlantic Ridge.

1. Introduction

Velocity measurements at the equator have different spectral contents for the two horizontal velocity components, with zonal motions dominated by longer periods than meridional motions. This behavior has been interpreted as being due to the presence of equatorial waves. Indeed, Kelvin and Rossby waves, which are the only wave candidates for long-period fluctuations, present small or vanishing meridional velocities on the equator (e.g., Philander 1978). As a result, at intermediate depths (600–1800 m) in the equatorial Atlantic, variability of the meridional velocity component is dominated by intraseasonal time scales while variability of the zonal velocity component is dominated by semiannual, annual, and interannual signals (e.g., Weisberg and Horigan 1981; Mercier and Speer 1998; Gouriou et al. 1999; Schmid et al. 2003; Thierry et al. 2004; Bunge et al. 2006).

At intermediate depths, observations and model results in the Atlantic indicate that both semiannual and annual signals are wind forced (Brandt and Eden 2005). These signals are the result of vertically propagating Rossby and Kelvin waves (e.g., Thierry et al. 2004). Interannual variability is not as well documented. At least part of the interannual variability has been related to the so-called equatorial deep jets (EDJs), for which

* Current affiliation: Department of Oceanography, The Florida State University, Tallahassee, Florida.

Corresponding author address: Lucia Bunge, Department of Oceanography, The Florida State University, Tallahassee, FL 32306-4320.
E-mail: bunge@ocean.fsu.edu

DOI: 10.1175/2008JPO3781.1

formation mechanisms are still not well understood. EDJs are characterized by vertically stacked alternating eastward and westward jets with small vertical scales (300–600 m) and amplitudes of the order of 10 cm s^{-1}. They are confined to a narrow equatorial band (of total width less than 3° latitude) and to depths between the thermocline and 2500 m (e.g., Firing 1987; Gouriou et al. 1999; Bourlès et al. 2003). The variability of EDJs is poorly documented. Since EDJs are embedded in larger vertical-scale currents, a single time series reflects the variability of a combination of different phenomena. To separate EDJ signals from larger vertical scale phenomena, long velocity time series (several years) with high vertical resolution are needed. The most complete dataset of EDJ direct measurements comes from the Line Islands Profiling (LIP) Project in the Pacific Ocean, which consists of 41 meridional sections of current velocities over 16 months at 159°W (Firing 1987). They found that some EDJs were nearly stationary during the 16 months while others were intermittent. They also found variations in the amplitude of EDJs that could not be attributed to the superposition of large vertical scale motions since adjacent jets were modulated together. They compared their results with velocity profiles from previous years, and concluded that jets in the Pacific did not propagate vertically at a uniform rate nor stay in place.

In the Atlantic, EDJs have also been observed to show multiple time scales and various types of temporal behavior, periodic and intermittent, depending on the location and the type of data analyzed. For example, Johnson and Zhang (2003), using hydrographic data from the center and west of the basin, suggested a periodic wavelike behavior with periods of at least 5 yr. Send et al. (2002), using four velocity time series of 24-month duration at 35°W, suggested an intermittent behavior of variable duration. A current meter array at 10°W provided 13 velocity time series of 13-month duration that were consistent with intermittent EDJs lasting a few months (Bunge et al. 2006). Thus, analyses of EDJ temporal characteristics in the Pacific and Atlantic have been hampered by the difficulty of collecting an appropriate dataset.

In the Atlantic, the zonal extent of EDJs has been estimated to reach at least 25°–27° (Gouriou et al. 2001; Schmid et al. 2005). These large zonal scales, along with their presumably long duration, turn EDJs into potentially important features in the equatorial zonal transport of water masses. However, estimating the transport of water masses along the equator by EDJs is difficult because the temporal nature of EDJs is still largely unknown (permanent, oscillatory, or intermittent).

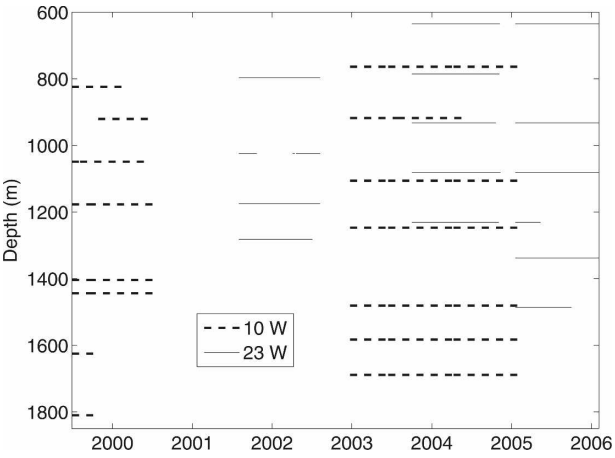

FIG. 1. Depth and time of the VACM at 10°W (dashed line) and at 23°W (continuous line). The *y* axis indicates depth, in meters; *x* axis indicates time, in years, with year labels centered at 15 May. The two sites were instrumented simultaneously from February 2004 to March 2005.

We present here long time series of high-vertical-resolution current meter measurements at intermediate depths (600–1800 m) at two locations on the equator, 10°W and 23°W. This extensive dataset provides additional insights into the temporal nature of EDJs and allows new estimates of the amplitude and phase of the annual and semiannual cycle at intermediate depths.

2. Data

The data consist of horizontal velocity measurements gathered by Vector Averaging Current Meters (VACMs) at intermediate depths at 23°W (635–1486 m) and at 10°W (764–1810 m). At 10°W, data were collected from November 1999 to November 2000 and then from May 2003 to June 2005. The current meter data from the year 2000 has been described partially in Bunge et al. (2006). At 23°W, data were collected from December 2001 to December 2002, from February 2004 to March 2005, and from May 2005 to June 2006. Thus, the two sites were instrumented simultaneously from February 2004 to March 2005 (Fig. 1).

The VACMs were calibrated both before and after deployment at the Institut Français de Recherche pour l'Exploitation de la Mer (IFREMER) in Brest, France, for velocity and pressure. The velocity accuracies are between ±1 and 2 cm s^{-1} for the various instruments, with the minimum measurable current speeds varying between 0.20 and 5.38 cm s^{-1}. The reported absolute pressure accuracies are of ±17, ±54, and ±60 dbar, depending on the pressure sensor scale range. Standard deviation for the pressure time series did not exceed 8

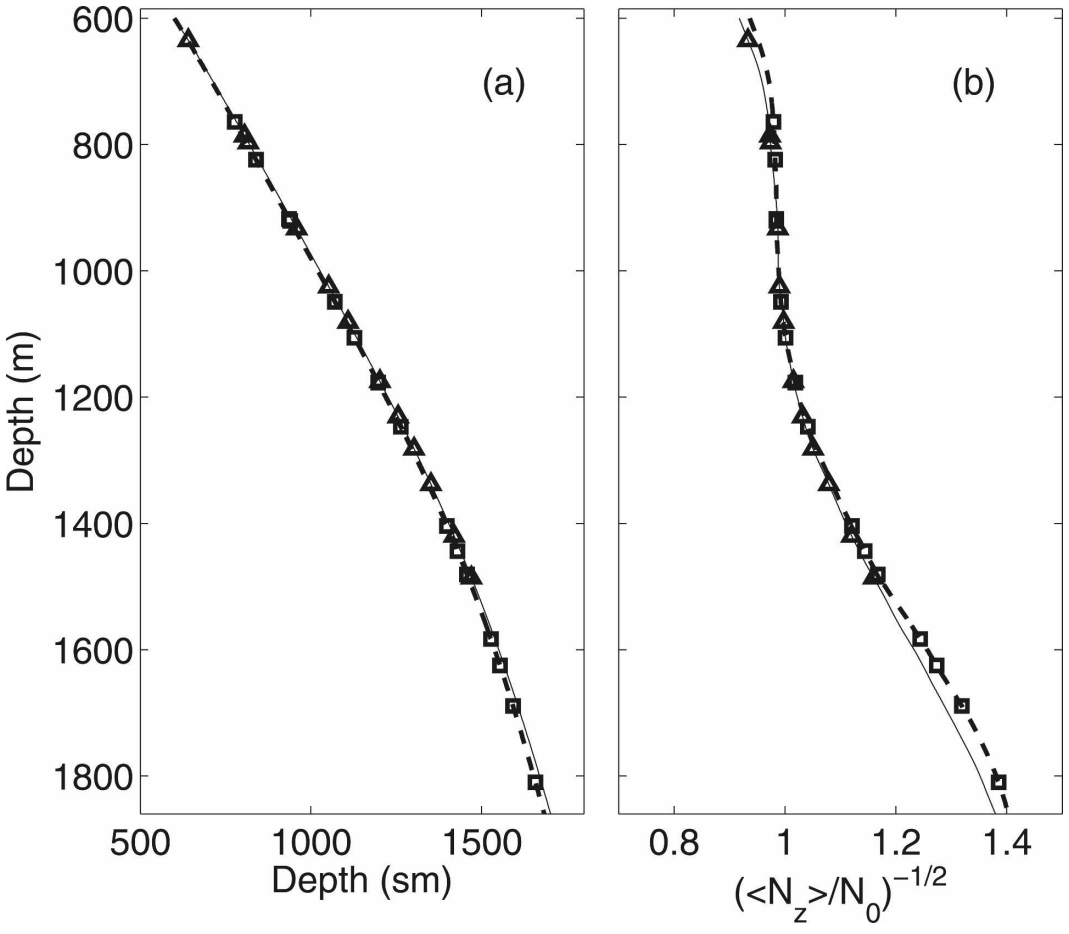

FIG. 2. (a) Stretched vertical coordinate as a function of depth at 23°W (continuous line) and at 10°W (dashed line). The relation between the original depth and the stretched depth is given by the differential law $dz_n = (\langle N(z)\rangle/N_0)dz$, where z and z_n are the original and the stretched depths, respectively. (b) Velocity scale factor $(\langle N(z)\rangle/N_0)^{-1/2}$ with depth at 23°W (continuous line) and at 10°W (dashed line). Here $\langle N(z)\rangle$ is the average Brunt–Väisälä frequency profile for the location, filtered with a 501-m running mean, followed by a 334-m running mean; N_0 is the reference Brunt–Väisälä frequency, equal to 2.37×10^{-3} s^{-1}. The normalized velocity is given by $u_n(z) = u(z)/(\langle N(z)\rangle/N_0)^{1/2}$ (after Leaman and Sanford 1975). The triangles and squares indicate the depth of the instruments at 23° and 10°W.

dbar. All of the moorings, with the exception of one of the two moorings in 2000, carried an upward-looking acoustic Doppler current meter profiler near the surface that detected the depth to the surface. This information, together with the information of the distance between instruments in the mooring line, allowed us to discard pressure outliers. More details on the data calibration and validation can be found in Kartavtseff (2003, 2004, 2006). The hourly data were averaged over 25 h to remove tidal frequencies and resampled to provide daily resolution.

Changes in the stratification of the water column modify the amplitude and the vertical scale of vertically propagating signals. To remove such effects, depths and velocities were scaled, using mean profiles of the Brunt–Väisälä frequency, as described in Leaman and Sanford (1975). The mean profiles of Brunt–Väisälä frequency were obtained from data collected during the Equalant program (see http://nansen.ipsl.jussieu.fr/EQUALANT). The differentiation of the vertical scale was made starting from 600 m. This choice of depth reduced the differences of the stretched-meter scale between 23° and 10°W (Fig. 2a). The Brunt–Väisälä frequency of reference is 2.37×10^{-3} s^{-1}, resulting in the velocity time series from the deepest positions getting multiplied by the largest scale factors (Fig. 2b); it is for these positions that the vertical scale in stretched meters between VACM becomes smaller, when compared to the distance in regular meters. The resulting scaled velocities in normalized centimeters per second

(hereafter ncm s^{-1}) at the different stretch-meter (sm) depths are presented in Figs. 3 and 4.

3. Zonal component

a. Semiannual and annual cycle

As mentioned in the introduction, observations have shown that EDJs are embedded in large vertical scale currents. One of the challenges in this study is to separate variability due to different types of phenomena, in particular, to separate variability having large vertical scale from variability due to EDJs, which have comparatively smaller vertical scales. The annual and semiannual cycles are considered to represent an important amount of the variability observed at the equator and at these depths (e.g., Schmid et al. 2003; Thierry et al. 2004) and have large vertical scales compared to EDJs. To evaluate the seasonal signal, two different approaches were followed. These methods were used separately at 10° and at 23°W because studies suggest that the seasonal signals affecting 10°W and 23°W belong to different meridional modes (Thierry et al. 2004, 2006).

Approach 1: A monthly climatology of the data was estimated at each location, 10° and 23°W. Because there is evidence that annual and semiannual signals present upward phase propagation (e.g., Brandt and Eden 2005; Thierry et al. 2006), we separated the data into three different depth ranges, obtaining three different climatologies per location. The three depth ranges were chosen arbitrarily by dividing the depth between the deepest and the shallowest VACM into three equal sections. The monthly values were composed of an average of 6 months of data (minimum of 4 months and maximum of 11 months). The advantage of climatologies is that, if enough information is used, they are very good approximations of the seasonal variability in a region; any phase locked signal, like annual and semiannual signals, is represented. The inconvenience of this method is that, because we choose three depth ranges at each location, some months at some levels have large confidence intervals (not shown). In addition, it is difficult to estimate characteristics of annual and semiannual waves, such as the vertical scale (or vertical phase speed) and amplitude from three climatologies.

Approach 2: Vertically propagating plane waves with semiannual and annual periods were fitted to the data using a least squares fit approach. The fitting was done by assuming a single plane wave for each period (annual and semiannual) at each location (10° and 23°W). The frequencies of the waves were fixed, but their vertical wavenumber, $m = 2\pi/L_z$, where L_z is the vertical scale of the wave, was allowed to change. The fitting is done over the entire dataset, considering all the series in one location as a single time series. Hence, this approach improves the confidence level in the annual and semiannual harmonics estimates because the fitting is done over very long time series (14.3 yr at 23°W and 19.8 yr at 10°W). The best fit, given by the waves representing the largest amount of variance in the series, gave two values of L_z, one for the annual harmonic and the other for the semiannual harmonic (Table 1). In addition, the amplitude of each harmonic was estimated through the coefficients of the fit (Wunsch 1996). The disadvantage of this approach is that it assumes a single signal of sinusoidal shape for each period.

When fitting a signal to data, one normally wants to represent most of the variance with the fitted signal and the residuals are considered noise. The uncorrelated residuals can then be used to estimate the confidence of the fitting. Here, the residuals contain the signal of EDJs and are definitely not uncorrelated. This is clear from the percentage of explained variance of each harmonic in Table 1. Therefore, the conventional way to estimate errors (e.g., Wunsch 1996) does not apply here. The reasoning for using a least squares fit approach is the following: we know a priori that an annual and semiannual signal exists in the data among other time scales of variability, and we choose the amplitude and vertical scale of the annual and semiannual signal that explains the largest amount of variance in the data. To test the sensitivity of the results, we examined the values of L_z (the vertical scale) that reduced by less than 1 ncm s^{-1} the amplitude of the signal, when compared to the maximum amplitude obtained with the best fit (see Table 1). Because the values of L_z are large when compared to the vertical extent of the measurements, the limits of L_z were only found for the low limit (i.e., no matter how large L_z was for a given wave, the amplitude of the wave was never smaller than 1 ncm s^{-1} of the best fitting wave).

The resulting curves from Approach 1 and 2 are shown in Figs. 3 and 4, superimposed to the data. At first glance, the two methods show that, at 23°W, the seasonal velocity variability is eastward in the first half of the year and westward in the second half of the year, in agreement with float data at 1000 m (Schmid et al. 2003). At 10°W, the flow is westward between April and October and eastward the rest of the year. The percentage of explained variance by the signals,

$$P = 1 - \frac{\mathrm{var}_{\mathrm{residuals}}}{\mathrm{var}_{\mathrm{data}}},$$

is similar in both approaches, approximately 30%. The similarities in amplitude and phase between the curves

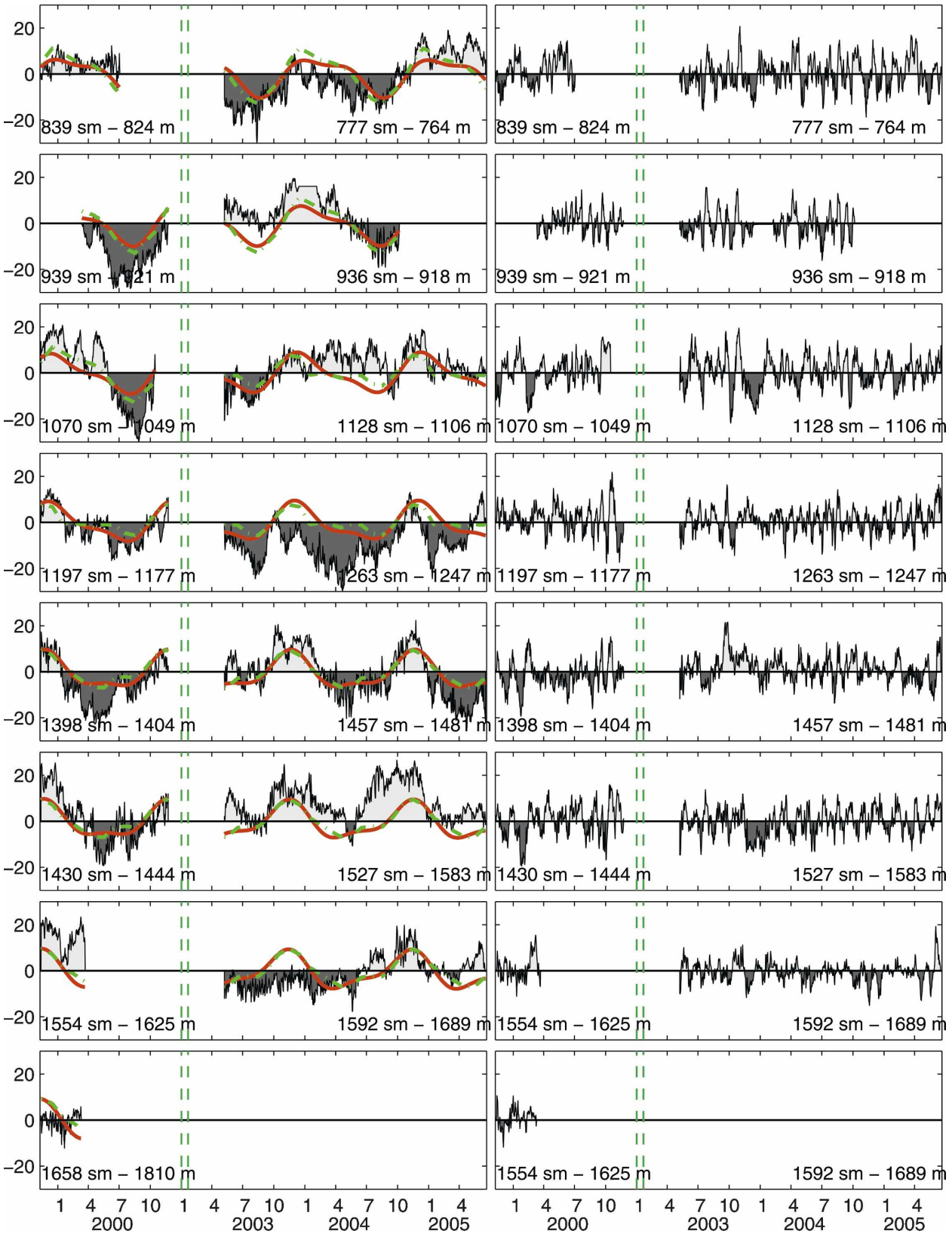

FIG. 3. Normalized velocity data from 10°W: (left) zonal velocity component. Superimposed to the zonal velocity data is the seasonal signal estimated using a climatology (green) and using a least squares fit (red). (right) Meridional velocity component. The depth of the instruments (in stretched meters and in meters) is indicated below each time series. The *y* axis indicates velocity (cm s^{-1}). The *x* axis indicates time in months from November 1999 to June 2005. Note that the time line is not linear; there is a gap in the data from November 2000 to May 2003 (dashed vertical lines). Depths of instruments in the same panel sometimes vary.

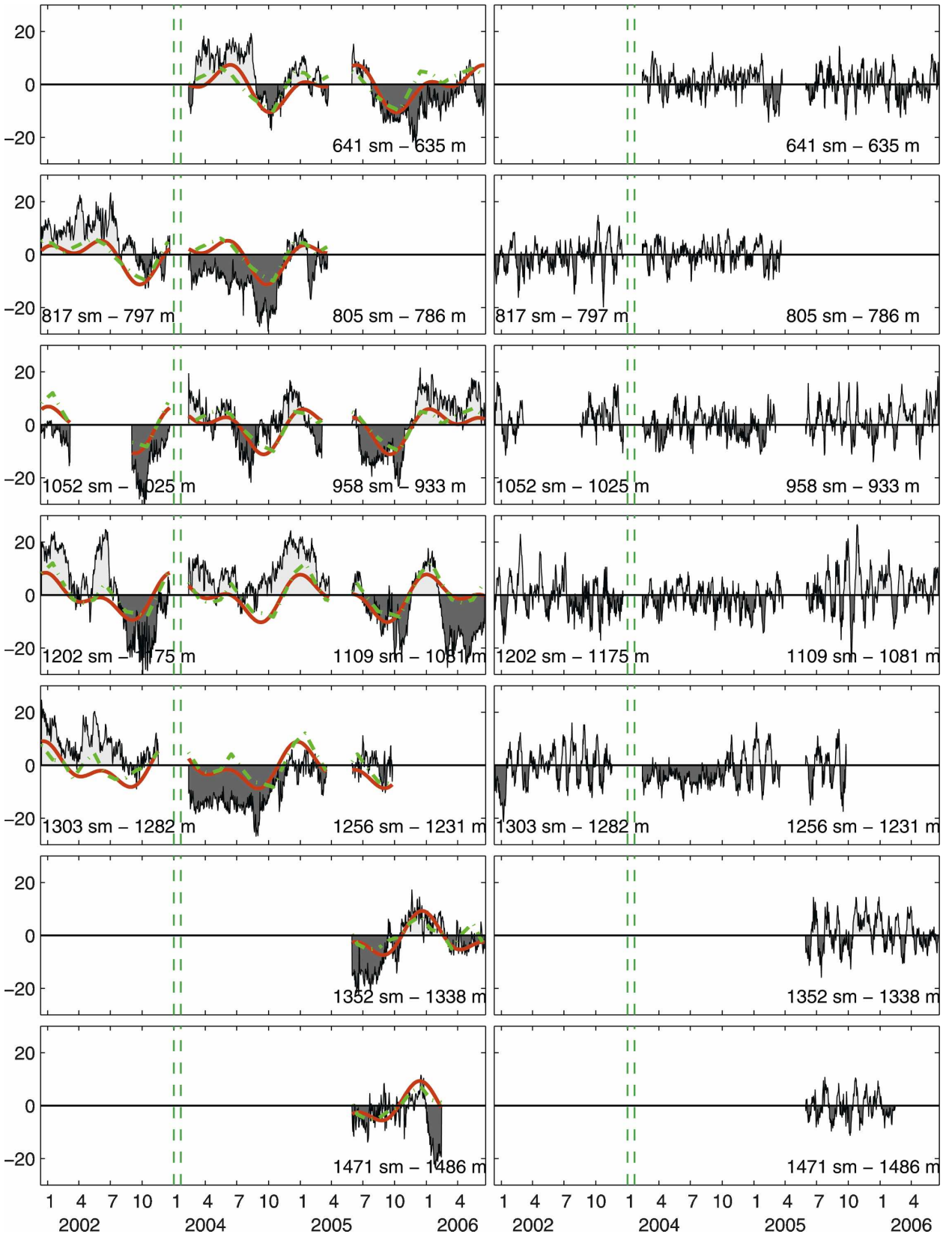

FIG. 4. As in Fig. 3, but from 23°W. The *x* axis indicates time in months from December 2001 to June 2006, and there is a gap in the data from December 2002 to February 2004.

TABLE 1. Best estimates of annual (A) and semiannual (S) harmonics: amplitude, vertical scale, and percentage of explained variance. The method assumes a plane wave with annual and semiannual periodicities and free vertical scale L_z for each harmonic. Thus, the best fit depends on the values of L_z. The sensitivity of the fitting is evaluated by examining the values of L_z that reduce the amplitude of the signal by less than 1 ncm s^{-1}, when compared to the amplitude of the best fit.

	23°W			10°W		
Period	Amplitude (ncm s^{-1})	Vertical scale (sm)	Percentage of explained variance	Amplitude (ncm s^{-1})	Vertical scale (sm)	Percentage of explained variance
S	4	$\rightarrow \infty$ $L_z > 1650$	8	3	$\rightarrow \infty$ $L_z > 1000$	4
A	6	2080 $L_z > 1100$	16	7	2550 $L_z > 1400$	25

of both approaches, especially at 10°W, suggest that both methods agree for a seasonal cycle with vertical scales larger than 1000 sm. Note that the shape of the curves varies with depth; this is due to the different vertical scales for annual and semiannual harmonics.

b. *Equatorial deep jets*

From the data at 10° and 23°W, one can infer the large vertical scale of the seasonal cycle from the smaller vertical scale of EDJs (Figs. 5a and 6a) and observe that the large eastward pulses at the depths of eastward jets are accompanied by a reduction of the westward velocity of the adjacent westward jets. The seasonal signal is significantly reduced when the climatologies are removed from the data (Figs. 5b and 6b) and the remaining signal is largely dominated by small vertical scale flows, characteristic of EDJs. We chose to remove the climatology instead of the plane waves because the climatology explained approximately 5% more of the variance and because, visually, it removed more of the large vertical scale variability. The following results are not changed if the plane wave with annual and semiannual harmonics is removed instead.

We then fitted a plane wave to the residuals using the entire dataset, with free parameters for vertical scale, zonal scale, and time scale. As for Approach 2 for the annual and semiannual harmonics, the sensitivity of the method was evaluated by examining the values of L_z (the vertical scale), P (the period), and L_x (the zonal scale) that reduce by less than 1 ncm s^{-1} the amplitude of the signal when compared to the amplitude of the best fit (Table 2). The best fit wave showed downward phase propagation, amplitude of 8 ncm s^{-1}, vertical scale of 440 sm, period of 4.4 yr, zonal scale of about 14° without clear direction of the zonal propagation (Table 2), and explained 53% of the variance in the velocity time series anomalies (see contours in Figs. 5b and 6b). The period of 4.4 yr is in the range of 5 ± 1 yr, the time scale found by Johnson and Zhang (2003) using hydrographic data. The vertical scale is in the smallest limit of values given by other authors [400–600 m, Gouriou et al. (1999); 400–700 sm, with a peek at 546 sm, Send et al. (2002); 661 sdbar, Johnson and Zhang (2003)]. It is important to mention that the characteristics of the 4.4-yr wave did not change if the fitting was done over the original data without removing the seasonal cycle. This suggests that the main seasonal and EDJ signals are not correlated and can be conveniently separated by the methodology used; we can see that, if we only remove the 4.4-yr wave from the original series, the velocity field is largely influenced by the seasonal signal (Figs. 5c and 6c) and the amount of explained variance by the seasonal signal increases to about 50%.

Following the same procedure used for the seasonal cycle, we extracted the 4.4-yr wave from the velocity anomalies (Figs. 5d and 6d). The flow patterns in the residual velocities were complicated, and we found again vertical scales and amplitudes in the range of EDJs. The velocity structure of the residuals shows that the 4.4-yr plane wave is not representing all of the variability of small vertical scales. For instance, variations in the intensity of the flows lasting only a few months were observed within the jets (Figs. 5b and 6b). Some of these variations cannot be attributed to the superposition of large vertical scale fluctuations since adjacent jets were modulated together. Over the entire dataset, the jets had a tendency to propagate downward. However, this propagation is not steady; there is even one instance in which the structure of the jets is not recognizable—the year 2000 at 10°W, between 1000 and 1400 sm—suggesting intermittence in the EDJ signal. The lower acoustic Doppler currentmeter profiler (LADCP) section at 10°W from the summer of 2000 confirms the disappearance of the jet structure at these depths (Gouriou et al. 2001). The different speeds of propagation, the erosion of the EDJ signal at specific depths, and the small vertical scale found for the best fitted wave when compared with other results can be

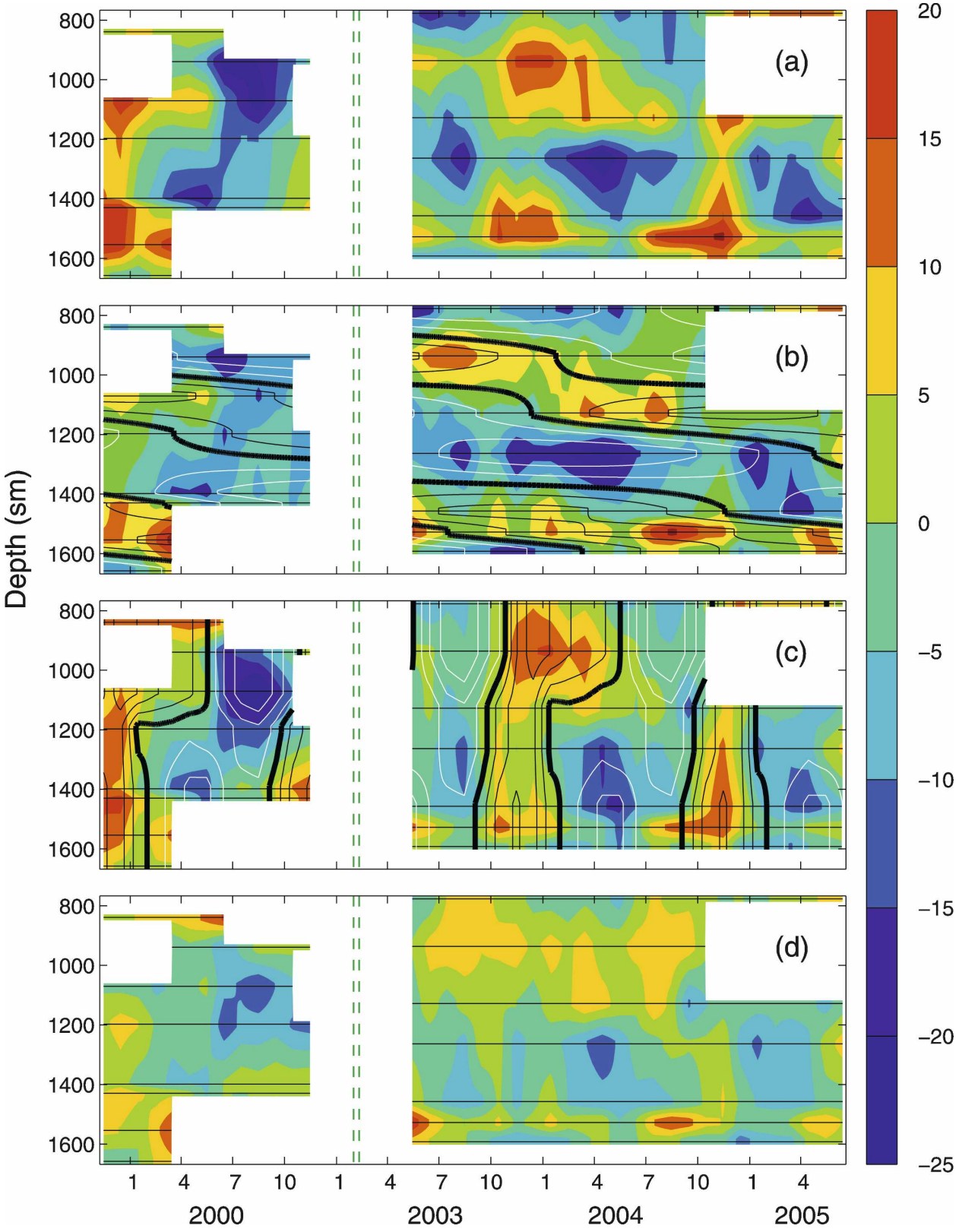

FIG. 5. Zonal velocity component (in ncm s^{-1}) at 10°W (a) before removing any signal, (b) after removing the seasonal cycle, (c) after removing the 4.4-yr period wave, and (d) after removing the seasonal cycle and the 4.4-yr period plane wave. Contours in (b) and (a) represent the 4.4-yr period plane wave and the climatology, respectively; in these contours the thick contour represents the zero velocity, and black and white contours represent positive and negative velocities. Horizontal black lines indicate where there is available data. The *y* axis indicates depth in sm. The *x* axis indicates time in months from November 1999 to June 2005. Note that the time line is not linear; there is a gap in the data from November 2000 to May 2003 (dashed vertical lines).

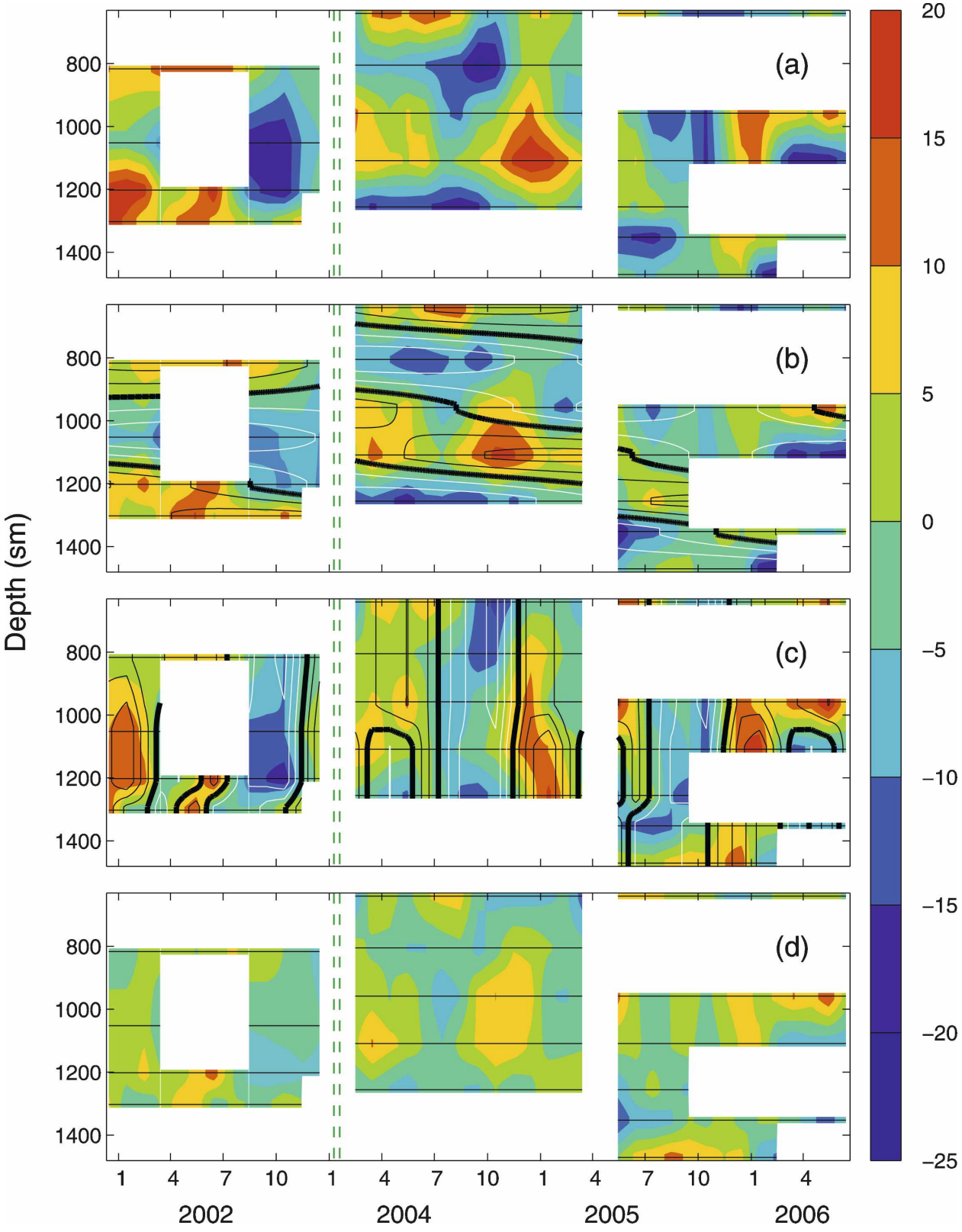

FIG. 6. As in Fig. 5, but at 23°W. The *x* axis indicates time in months from December 2001 to June 2006, and there is a gap in the data from December 2002 to February 2004.

TABLE 2. Characteristics of the wave that best fit the residual data (once the seasonal cycle was removed). The sensitivity of the fitting is evaluated by examining the values of P, L_z, and L_x that reduce by less than 1 ncm s^{-1} the amplitude of the signal, when compared to the amplitude of the best fit.

Period (yr)	Amplitude (ncm s^{-1})	Vertical scale (sm)	Zonal scale
4.4 with $3.7 < P < 5.2$	8	440 with $360 < L_z < 520$	14° with $11° < L_x < 18°$

interpreted as the simultaneous occurrence of different signals with vertical scales in the range of EDJ signals. Furthermore, the direction of the flow at the instrument's depths changed over the time of measurements, except at around 1500 sm where only eastward flows were observed, suggesting that multiple time scales for jetlike structures at different depths are possible (Figs. 5d and 6d). A semipermanent eastward jet at around 1500 sm had already been suggested by Andrié et al. (2002), who found eastward velocities and a maximum of chlorofluoromethanes, a tracer of North Atlantic Deep Water at this depth. The 1500-sm depth flow is surmised to be part of the bifurcation of the deep western boundary current to the east at the equator, which transports Upper North Atlantic Deep Water at least as far as 5°W along the equatorial Atlantic (Messias et al. 1999).

4. Meridional velocity component

The meridional velocity component at both locations is dominated by quasiperiodic intraseasonal fluctuations that are sometimes modulated in time and sometimes occur only in certain portions of a time series (see Figs. 3 and 4). To evaluate the period, the seasonality, and the possible variation of the period range with depth of these signals, we used a wavelet–ridge analysis technique (Delprat et al. 1992; Mallat 1999) together with a reconstruction scheme. The complete procedure is explained in detail in Bunge et al. (2006). In brief, the technique consists of isolating all ridges from each wavelet transform. Each point in the ridge has an instantaneous frequency, amplitude, and time of occurrence. This information permits the reconstruction of signals as well as a statistical evaluation of the variability in the time series.

Quasiperiodic fluctuations in the meridional velocity component at intermediate depths were separated into five bands: 5–10 days, 10–20 days, 20–45 days, 45–70 days, and 70–90 days (Fig. 7). Overall, the most common oscillations had a period between 20 and 45 days. To evaluate if there were any differences in the depths at which these period bands were found, we separated the ridge information into three depth groups. The three depth ranges were chosen arbitrarily by dividing the depth between the deepest and the shallowest VACM into three equal sections. The only oscillations having a gradual decrease in events with depth were the ones in the 10–20-day period band (Fig. 8, top panel). The reduction in the number of these waves with depth suggested a possible near-surface origin. Extraction and localization of the signals in time indicated that all four period bands were found throughout the year. Nonetheless, there are certain times in the year when certain periods were more common than others. For example, fluctuations in the 10–20-day band were more common during boreal spring and summer and oscillations in the 20–45-day band were more common in late boreal summer and autumn (Fig. 8, bottom panel). A similar relation between period band and seasonality is found near the surface (Bunge et al. 2006, 2007), suggesting that 10–20-day period oscillations and some of the 20–45-day period oscillations are forced close to the surface.

Although periods less than 45 days dominated the

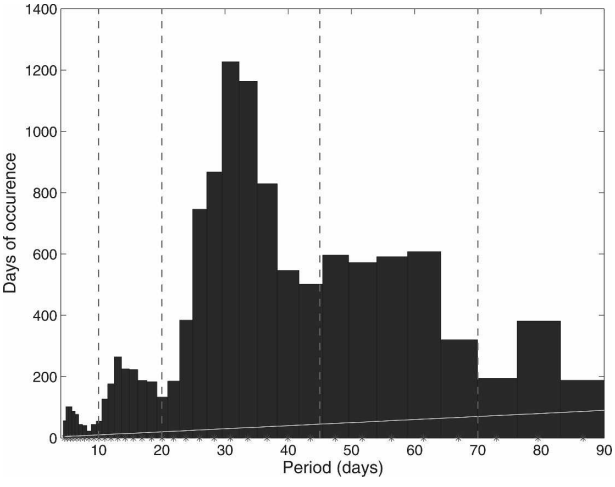

FIG. 7. Ridge histograms for the meridional velocity components of all current meter data. The bins were constructed by choosing the inverse of the central frequency of the wavelets used to calculate the wavelet transform. Central frequencies of the wavelets follow a logarithmic progression in such a way that $\Delta \log f = \text{const}$; therefore, bins from long periods are larger than those of short periods. The vertical dotted lines indicate the limits of period bands considered (5–10, 10–20, 20–45, 45–70, and 70–90 days). The white line indicates the portion of the bars equivalent to one cycle.

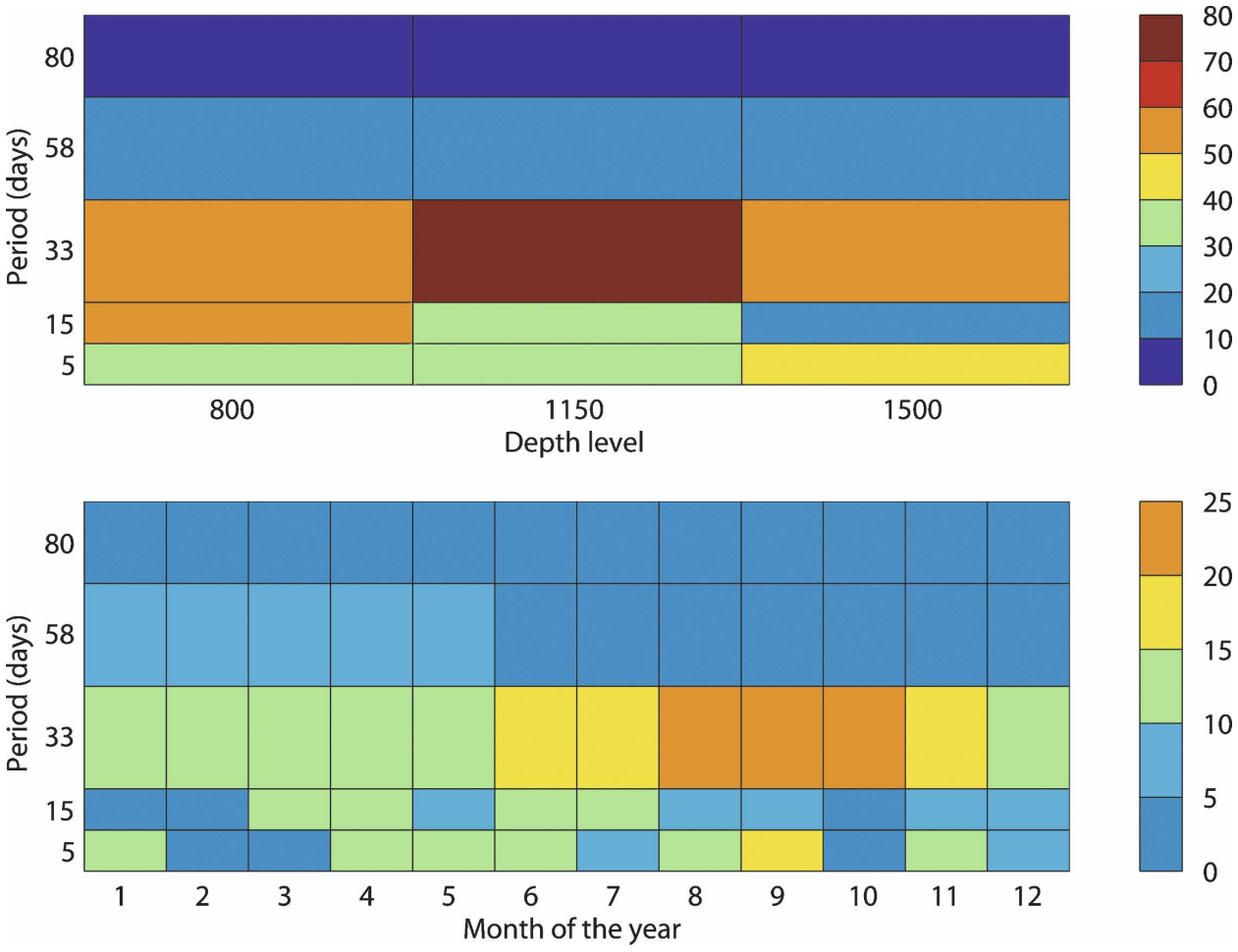

FIG. 8. Number of oscillations in the meridional velocity component as a function of their (top) period band and depth level; the *x* axis represents the approximate central depths of the three levels in sm; and (bottom) period band and occurrence in the months of the year; the *x* axis indicates the month of the year. In both graphs, the ridge data was separated by period range and subsequently by (top) depth level and (bottom) month of the year. The *y* axis in both graphs indicates the period of the bands (defined from the histogram in Fig. 7). The color scale indicates the number of oscillations of the period bands present on each level/month.

variations in the meridional velocity component at both locations, at 23°W the velocity record at 1231 m showed continuous southward velocities for over 7 months during 2004 (Fig. 3). In fact, all meridional velocities at 23°W during 2004 were subject to low frequency fluctuations. One of the differences between 10° and 23°W is the presence of the Mid-Atlantic Ridge at 23°W. McPhaden and Gill (1987) studied the scattering of low-frequency equatorial Kelvin wave energy by a submarine ridge. They found that the presence of a submarine ridge in the path of propagation of a Kelvin wave induced meridional motions. The model that they used was of very low vertical resolution and their results cannot be directly compared with these data. Nonetheless, we suggest that more work along the lines of McPhaden and Gill (1987) may be able to explain the low frequency fluctuations observed in the meridional component at 23°W.

5. Discussion

The difficulties in establishing an appropriate time scale for assessing the variation in the parameters of EDJs through observations reside in the lack of long time series of data with high vertical resolution. The moorings at 10° and at 23°W provided the velocity time series with the longest duration and high vertical resolution for the depths sampled at the equator. The seasonal cycle from the climatology together with a 4.4-yr plane wave of small vertical scale can explain 74% of the variance in the zonal velocity component. However, the residuals and a close examination of the data sug-

gest that, along with the 4.4-yr wave, there are other features of small vertical scale coexisting with a seasonal cycle of a much larger vertical scale. Thus, in a given time series, the signal of a given EDJ pattern is not only aliased by the annual signal but also by other EDJ-like signals presenting different vertical patterns and/or time scales. From this perspective, the velocity snapshot profiles used in numerous EDJ studies represent a mean of a combination of all EDJ forms during the measurement period.

There is no evidence that EDJs or EDJ-like structures in the Atlantic have a net zonal mass transport, but the complexity of their vertical and temporal structure (i.e., intermittence and different depth-dependent time scales) suggests that interdecadal zonal transport variability due to EDJs is plausible. That question will have to be addressed by realistic numerical models capable of representing the complex characteristics observed in the EDJ system.

A numerical model (D'Orgeville et al. 2007) based on a recent theory of the mechanism of EDJ formation (Hua et al. 2008) provides evidence that the instability of mixed Rossby–gravity waves at the equator, forced by the deep western boundary current may trigger small vertical-scale zonal flows. In the model results presented by D'Orgeville et al., the vertical scale of the jets depends on the period of the mixed Rossby–gravity wave, which in their Atlantic simulation is ~60 days. They also found that the structure of the jets can have a standing-mode pattern or a vertical propagating pattern (upward or downward), depending on the amplitude of the excited mixed Rossby–gravity wave. The time scales of these EDJs corresponded roughly to equatorial basin modes (~5 yr in the Atlantic for a first equatorial basin mode of vertical number 20); however, the basin modes may also present horizontal patterns corresponding to a second or higher equatorial basin mode, in which cases the period would be drastically reduced (e.g., ~2.5 yr for the second equatorial basin mode). This model is quite idealized: the geometry of the basin is rectangular with flat bottom; the Brunt–Väisälä frequency is constant (no thermocline or differences in water masses); and the forcing is monochromatic in time (one single period per run) and in space (one single vertical mode per run). Nonetheless, due to the formation mechanisms proposed, it suggests that a wide range of EDJ signals is possible.

Acknowledgments. This research was funded by the French national PATOM program (Programme Atmosphère et Océans Multi-échelles). We thank the crew of the R/V *Atalante* (both mooring deployment at 23°W and mooring recovery and redeployment at 10°W), the crew of the R/V *Beautemps-Beaupré* (first mooring deployment at 10°W), the crew of the R/V *Le Suroit* (mooring recovery), and the crew of *Meteor* (mooring recovery at 23°W) for their excellent cooperation. We would also like to thank one of the anonymous reviewers for suggesting the use of plane waves to analyze the data, and Kevin Speer, Irene Garcia, Leif Thomas, Jonathan Lilly, and William Dewar for their stimulating discussions.

REFERENCES

Andrié, C., M. Rhein, S. Freudenthal, and O. Plahn, 2002: CFC time series in the deep water masses of the western tropical Atlantic, 1990-1999. *Deep-Sea Res. I,* **49,** 281–304.

Bourlès, B., and Coauthors, 2003: The deep currents in the Eastern Equatorial Atlantic Ocean. *Geophys. Res. Lett.,* **30,** 8002, doi:10.1029/2002GL015095.

Brandt, P., and C. Eden, 2005: Annual cycle and interannual variability of the mid-depth tropical Atlantic Ocean. *Deep-Sea Res. I,* **52,** 199–219.

Bunge, L., C. Provost, J. M. Lilly, M. D'Orgeville, A. Kartavtseff, and J.-L. Melice, 2006: Variability of the horizontal velocity structure in the upper 1600 m of the water column on the equator at 10° W. *J. Phys. Oceanogr.,* **36,** 1287–1304.

——, ——, and A. Kartavtseff, 2007: Variability in horizontal current velocities in the central and eastern equatorial Atlantic in 2002. *J. Geophys. Res.,* **112,** C02014, doi:10.1029/2006JC003704.

Delprat, N., B. Escudié, P. Guillemain, R. Kronland-Martinet, P. Tchamitchian, and B. Torrésami, 1992: Asymptotic wavelet and Gabor analysis: Extraction of instantaneous frequencies. *IEEE Trans. Inf. Theory,* **38,** 644–665.

D'Orgeville, M., B. L. Hua, and H. Sasaki, 2007: Equatorial deep jets triggered by a large vertical scale variability within the western boundary layer. *J. Mar. Res.,* **65,** 1–25.

Firing, E., 1987: Deep zonal currents in the central equatorial Pacific. *J. Mar. Res.,* **45,** 791–812.

Gouriou, Y., B. Bourlès, H. Mercier, and R. Chuchla, 1999: Deep jets in the equatorial Atlantic Ocean. *J. Geophys. Res.,* **104** (C9), 21 217–21 226.

——, and Coauthors, 2001: Deep circulation in the Equatorial Atlantic Ocean. *Geophys. Res. Lett.,* **28,** 819–822.

Hua, B. L., M. D'Orgeville, C. Menesguen, and H. Sasaki, 2008: Destabilization of mixed Rossby-gravity waves and equatorial zonal jets formation. *J. Fluid Mech.,* in press.

Johnson, G. C., and D. Zhang, 2003: Structure of the Atlantic Ocean equatorial deep jets. *J. Phys. Oceanogr.,* **33,** 600–609.

Kartavtseff, A., 2003: Mouillages courantométriques PIRATA 10°W et 23°W. LODYC Internal Rep. 2003-01, 132 pp.

——, 2004: Mouillage courantométrique PIRATA 10°W. LODYC Internal Rep. 2004-01, 116 pp.

——, 2006: Mouillages courantométriques PIRATA 10°W et 23°W. LODYC Internal Rep. 2006-01, 210 pp.

Leaman, K. D., and T. B. Sanford, 1975: Vertical energy propagation of inertial waves: A vector spectral analysis of velocity profiles. *J. Geophys. Res.,* **80,** 1975–1978./

Mallat, S., 1999: *A Wavelet Tour of Signal Processing.* 2nd ed. Academic Press, 637 pp.

McPhaden, M. J., and A. E. Gill, 1987: Topographic scattering of equatorial Kelvin waves. *J. Phys. Oceanogr.,* **17,** 82–96.

Mercier, H., and K. G. Speer, 1998: Transport of bottom water in the Romanche Fracture Zone and the Chain Fracture Zone. *J. Phys. Oceanogr.,* **28,** 779–790.

Messias, M.-J., C. Andrié, L. Memery, and H. Mercier, 1999: Tracing the North Atlantic Deep Water through the Romanche and Chain fracture zones with chlorofluoromethanes. *Deep-Sea Res. I,* **46,** 1247–1278.

Philander, S. G. H., 1978: Forced oceanic waves. *Rev. Geophys. Space Phys.,* **16,** 15–46.

Schmid, C., Z. Garraffo, E. Johns, and S. L. Garzoli, 2003: Pathways and variability at intermediate depths in the tropical Atlantic. *Interhemispheric Water Exchange in the Atlantic Ocean,* G. Goni and P. Malanotte-Rizzoli, Eds., Elsevier, 233–268.

——, B. Bourlès, and Y. Gouriou, 2005: Impact of the equatorial deep jets on estimates of the zonal transports in the Atlantic. *Deep-Sea Res. II,* **52,** 409–428.

Send, U., C. Eden, and F. Schott, 2002: Atlantic equatorial deep jets: Space–time structure and cross-equatorial fluxes. *J. Phys. Oceanogr.,* **32,** 891–902.

Thierry, V., A. M. Treguier, and H. Mercier, 2004: Numerical study of the annual and semi-annual fluctuations in the deep equatorial Atlantic Ocean. *Ocean Modell.,* **6,** 1–30.

——, ——, and ——, 2006: Seasonal fluctuations in the deep central equatorial Atlantic Ocean: A data-model comparison. *Ocean Dyn.,* **56,** 581–593.

Weisberg, R. H., and A. M. Horigan, 1981: Low-frequency variability in the equatorial Atlantic. *J. Phys. Oceanogr.,* **11,** 913–920.

Wunsch, C., 1996: *The Ocean Circulation Inverse Problem.* Cambridge University Press, 442 pp.